Analytical Methods

Accepted Manuscript

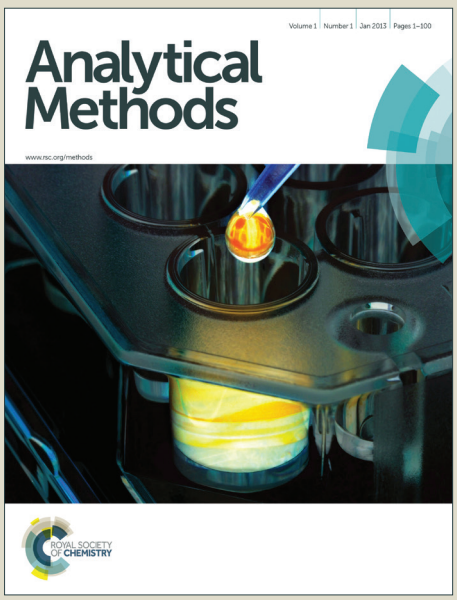

ROYAL SOCIETY OF CHEMISTRY

www.rsc.org/methods

Analytical Methods

RSCPublishing

ARTICLE

Amino-functionalized Silica-encapsulated Mn/ZnS Quantum Dots for the Room-Temperature Phosphorescence Determination of Graphene Oxide in Environmental Water Samples

Cite this: DOI: 10.1039/xoxxoooooox

Received ooth January 2012,
Accepted ooth January 2012

DOI: 10.1039/xoxxoooooox

www.rsc.org/

Yaping Zhong, [b] Qingpu Wang, [b] Yu He, *[a, b] Yili Ge, [a, b] Gongwu Song [a, b]

We developed a simple and sensitive room-temperature phosphorescence (RTP) method for the determination of graphene oxide (GO) in environmental water samples using amino-functionalized silica-encapsulated Mn/ZnS Quantum Dots ($Mn/ZnS@SiO_2$-NH_2) as a phosphorescence probe. The maximum phosphorescence excitation and emission wavelength of synthesized $Mn/ZnS@SiO_2$-NH_2 nanoparticles were 320 nm and 595 nm. The RTP intensity of $Mn/ZnS@SiO_2$-NH_2 nanoparticles could be quenched in the presence of GO with a detection limit as low as 1.0 $mg \cdot L^{-1}$. Good linear correlations were obtained over the concentration range from 0 to 10.0 $mg \cdot L^{-1}$ with a correlation coefficient of 0.9987, 10.0 to 25.0 $mg \cdot L^{-1}$ with a correlation coefficient of 0.9979. The phosphorescence quenching mechanism was also discussed. This method was successfully applied to the determination of GO in environmental water samples which presages more opportunities for application in biological and environmental systems.

Introduction

Graphene oxide (GO) is a single-atomic-layered material similar to graphite with its base having oxygen-containing groups and has a unique structure composed of sp^2 carbons surrounded by sp^3 carbons, [1] which confer it an excellent aqueous solubility, surface functionalizability and fluorescence quenching ability. [2] Thus, GO has been widely used as a sensor for the detection of metal ions, proteins and biomolecules. [3-5] Owing to the great hydrophilicity and solubility of GO, they could contaminate the soil, surface and underground water and consequently enter the ecosystem, if left in environment. The toxicological effects of GO have been evaluated. It has been demonstrated that GO is able to penetrate through membrane, altering cell morphology, inducing membrane damage and oxidative stress in adenocarcinoma human cells. [6] Furthermore, the toxicity, genotoxicity and cytotoxicity of GO have been reported in human and animal cells, immune cells and blood components. [7-10] In vivo studies in mice showed that GO can be accumulated in lungs liver and spleen. [11] With the increasingly production and use of graphene and graphene-family nanomaterials, it is necessary to evaluate their influence on the environment and subsequently, on the ecosystem health, including humans. However, there are only limited analytical methodologies focused on the detection and quantification of engineered nanomaterials, in spite of some approaches that have been developed in case of metallic nanoparticles [12-13] and carbon nanotubes [14-16]. Therefore, it is of great significance to develop sensitive, selective and flexible methods for the detecting of GO.

Semiconductor nanocrystals, known as quantum dots (QDs), have attracted much interest on account of their unique optical properties such as high luminescence efficiency [17], continuous excitation spectrum, high stability against photobleaching, controllable and narrow emission bands [18]. While most researches concentrated on the development of fluorescence of QDs-based fluorescence sensors, much less attention is paid to the phosphorescence properties of QDs and their potential as phosphorescence sensors. [19] Room-temperature phosphorescence (RTP) detection owns many advantages over fluorescence method. The long lifetime of phosphorescence allows an appropriate delay time, so that any fluorescence emission and scattering light can be easily avoided. The selectivity is enhanced because it is a less usual phenomenon than that of fluorescence. [20] The delayed luminescence lifetimes of dopants and host semiconductors have been studied in a number of doped semiconductor systems. [21-23] Doped semiconductors have also been employed as phosphor powders for colour displays. [24–26] Nevertheless, QDs have seldom been explored for RTP detection in aqueous solution. [27]

Herein, we introduced Mn/ZnS@SiO_2-NH_2 as a phosphorescence probe for the determination of GO in environmental water samples by RTP technology. To the best of our knowledge, ZnS QDs-based hybrid nanospheres as a phosphorescence probe for the detection of GO in environmental water samples have not been reported so far.

Experimental

Reagents

All chemicals used were of at least analytical grade. L-cysteine, zinc acetate dihydrate (Zn $(CH_3COO)_2 \cdot 2H_2O$), sodium nitrate ($NaNO_3$) and hydrogen peroxide (H_2O_2) were purchased form Sinopharm Chemical Reagent Co., LTD (Shanghai, China). Sodium sulfide (Na_2S) and (3-aminopropyl) triethoxysilane (APTES) were purchased from Aladdin Reagent Co., Ltd., China. Tetraethyl orthosilicate (TEOS), sodium hydroxide (NaOH) and ethanol absolute were purchased from Bodi Chemical Co., LTD (Tianjin, China). Powdered flake graphite (325 mesh) and Potassium permanganate ($KMnO_4$) were purchased from Asbury Carbons Ltd. (Shanghai, China) and Jiaozuo Chemical Plant (Henan, China), respectively. Ammonia solution ($NH_3 \cdot H_2O$) and sulfuric acid (H_2SO_4) were purchased from Kaifeng Dongda Chemical Plant (Henan, China). Milli-Q water (18 MΩ cm) was used throughout the experiments. All chemicals were used as received without further purification.

Instruments

Room-temperature phosphorescence (RTP) intensity was recorded on a LS55 fluorescence spectrometer (Perkin-Elmer, America). The TEM images of the prepared samples were examined using a TecnaiG20 transmission electron microscope (FEI, American). Fourier Transform Infra-Red (FTIR) spectra were taken with a spectrum one FTIR spectrophotometer (Perkin-Elmer, America) at room temperature. XRD patterns were examined by a D/max-IIIC X-ray diffractometer (Shimadzu, Japan)

Synthesis of L-cysteine-capped Mn-Doped ZnS QDs (Mn/ZnS QDs)

The preparation of L-cysteine-capped Mn-Doped ZnS QDs were performed according to previous methods with some modifications. [28] Typically, to a three-necked flask, 50 mL of 0.02 M L-cysteine, 5 mL of 0.1 M $Zn(CH_3COO)_2$, and 1.5 mL of 0.01 M $MnCl_2$ were added. The mixed solution was adjusted to pH 11 with 1 M NaOH and stirred under nitrogen environment at room temperature for 30 min. Then 5 mL of 0.1 M Na_2S was quickly injected into the solution. The mixture was stirred for 20 min, and then the solution was aged at 50 °C under air for 2 h to form Mn/ZnS QDs.

Encapsulation of Mn/ZnS QDs in SiO_2 spheres Mn/ZnS QDs were loaded inside silica nanoparticles based on a modified Stober method. [29] Briefly, 40 mL of ethanol, 8 mL of Mn/ZnS QDs solution and 0.4 mL of ammonia (28 wt %) were mixed under stirring in a 100 mL flask, and then 100 μL TEOS was added to the system quickly. The reaction was allowed to continue for 2 h with moderate stirring at 25 ℃. The obtained SiO_2 spheres containing Mn/ZnS QDs were subjected to three cycles of precipitation by centrifugation and washed with ethanol to remove the excess reactants.

Synthesis of the amino-functionalized Mn/ZnS@SiO_2 (Mn/ZnS@SiO_2-NH_2)

The above obtained Mn/ZnS@SiO_2 spheres were used as seeds for the growth of a second layer of silica with amino groups. The Mn/ZnS@SiO_2 spheres were added to 30 mL of ethanol, and 0.4 mL of ammonia (28 wt %) were added under stirring, then 100 μL TEOS and 100 μL APTES were added and reacted for 4 h. The products were subjected to three cycles of precipitation by centrifugation and washed with ethanol to remove the excess reactants.

Synthesis of Graphene Oxide (GO)

GO was synthesized from graphite via a modified Hummers and Offeman's method. [30-32] 1.0 g of powdered flake graphite and 0.5 g of $NaNO_3$ were taken in 500 mL round bottom flask, followed by addition of 3 mL of conc. H_2SO_4. Then 3.0 g of $KMnO_4$ was added slowly to the mixture in an ice-bath, to avoid rapid heat evaluation. After 2 hours the reaction mixture was allowed to stir at 35 °C for 30 minutes. Finally, the reaction mixture was added to 50 mL of water allowed to stir at 98 °C for 30 minutes, which results change of color of the mixture from yellow to brown. Then 85 mL of water was allowed to stir, and the reaction was ended by the addition of 4 mL of 30% H_2O_2. The warm solution was then filtered and subjected to three cycles of precipitation by centrifugation and washed with 5% HCl and then dialyzed using 3000 Da MWCO dialysis bag in de-ionized water for 48 h. The dry product was dissolved in water ultrosonicated to exfoliate oxidized graphene.

Results and discussion

Characterization of Mn/ZnS@SiO_2-NH_2.

We synthesized the Mn/ZnS@SiO_2-NH_2 nanospheres as illustrated in Scheme 1. In the first step, L-cysteine-capped Mn-

doped ZnS QDs (Mn/ZnS QDs) were encapsulated into silica to form the uniform Mn/ZnS@SiO_2 particles. Then the as-prepared ZnS@SiO_2 were silanized with 3-amimopropyltriethoxysilane (APTES) to prepare another layer of silica with amino on the surface (Mn/ZnS@SiO_2-NH_2).

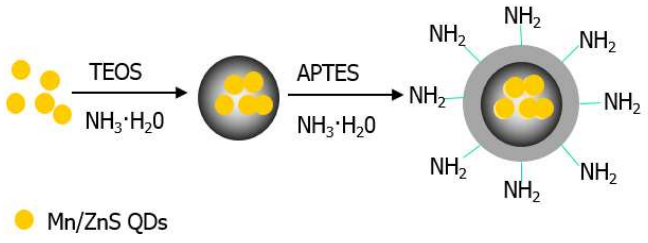

Scheme 1. Illustration of the procedure of preparing of the Mn/ZnS@SiO_2-NH_2.

The morphology of the Mn/ZnS@SiO_2-NH_2 was studied by transmission electron microscopy (TEM). As shown in Figure 1a, the size of the original Mn/ZnS QDs was about 5 nm. The as-prepared Mn/ZnS@SiO_2 nanoparticles were close to spherical, aggregated, with diameters ranging from 70 to 120 nm (Figure 1b to Figure 1c). After a second layer of silica shell modification, the Mn/ZnS@SiO_2-NH_2 nanoparticles were monodispersed with an average size of around 600 nm (Figure 1d).

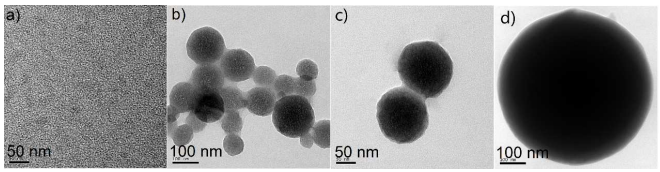

Figure 1. TEM images of the a) Mn/ZnS QDs, b) Mn/ZnS@SiO_2, c) Mn/ZnS@SiO_2 and d) Mn/ZnS@SiO_2-NH_2.

Figure 2 showed the FTIR spectra of Mn/ZnS QDs, Mn/ZnS@SiO_2 and Mn/ZnS@SiO_2-NH_2 and the phosphorescence spectrum of the Mn/ZnS@SiO_2-NH_2. As shown in Figure 2a (I), the IR absorption peaks at around 1591.2 cm^{-1} and 1398.5 cm^{-1} indicated the $-COO^-$ group. The peak at 3238.0 cm^{-1} indicated the $-NH_2$ group. According to the Kho et al.'s [33] ligand competition mechanism, L-cysteine can bind with ZnS by covalent bonds and form L-cysteine-capped Mn/ZnS QDs. The mercapto group of L-cysteine can bind to the sulfur atom of the ZnS QDs, and polar carboxylic acid group rendered the nanoparticles water-soluble. Therefore, carboxylic acid and amino group were presented on the surface of the ZnS QDs, while the S–H group vibration (2550–2670 cm^{-1}) was absent on the surface of the Mn/ZnS QDs. As shown in Figure 2a (II), the absorption peak at 1090.5 cm^{-1} was originated from the Si–O–Si stretching vibration of the SiO_2 shell. Besides, Mn/ZnS QDs were successfully encapsulated in the silica sphere because the absorption band at 3500–3000 cm^{-1} was much weaker compared with that of the original Mn/ZnS QDs. While after the Mn/ZnS@SiO_2 nanoparticles were amino-functionalized, the absorption peak at 3347.2 cm^{-1} suggested the $-NH_2$ group present on the surface of Mn/ZnS@SiO_2 (Figure 2a (III)) which further confirmed the successful synthesis of amino-functionalized silica-encapsulated Mn/ZnS Quantum Dots. The maximum phosphorescence excitation and emission wavelength of synthesized Mn/ZnS@SiO_2-NH_2 nanoparticles were 320 nm and 595 nm Figure 2b.

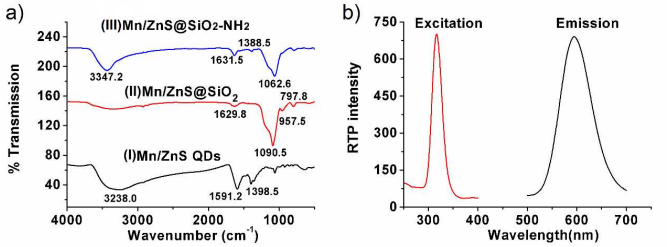

Figure 2. a) FTIR spectra of the (I) Mn/ZnS QDs, (II) Mn/ZnS@SiO_2 and (III) Mn/ZnS@SiO_2-NH_2. b) Phosphorescence spectrum of the Mn/ZnS@SiO_2-NH_2.

Characterization of GO

The protocol for preparing GO was synthesized from graphite via a modified Hummers and Offeman's method, which can be characterized by X-ray diffraction (XRD) and Fourier transform infrared spectroscopy (FTIR). The diffraction angle 2θ at 10.94° (Figure 3a) demonstrated the successful synthesis of GO [34-35]. The FTIR of GO further provided the information of the successful synthesis of GO. As shown in Figure 3b, the FTIR spectrum gave the characteristic vibrations of GO, as those reported in previous work [36], including a broad and intense peak of O—H group at 3439 cm^{-1}, a C=O peak at 1725 cm^{-1}, an O—H deformation peak at 1394 cm^{-1}, a C—OH stretching peak at 1261 cm^{-1}, an C—O stretching peak at 1060 cm^{-1}, and a peak attributed to the vibrations of unoxidized graphitic skeletal domains and the adsorbed water molecules at 1625 cm^{-1}.

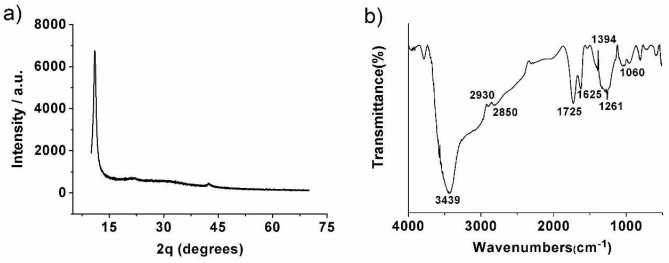

Figure 3. a) XRD pattern and b) FTIR spectrum of GO.

Feasibility of Mn/ZnS@SiO_2-NH_2 for the detection of GO.

The influence of pH on the phosphorescence quenching efficiency of the sensor by GO was evaluated (Figure 4a). When the GO solution was mixed with the Mn/ZnS@SiO_2-NH_2 solution at pH 7.4, the highest quenching effect was observed. Thus, pH 7.4 was selected as the optimal pH for the following experiments.

The RTP intensity of Mn/ZnS@SiO_2-NH_2 was decreased with the increase of the concentration of GO (Figure 4b). The RTP emissions of Mn/ZnS@SiO_2-NH_2 at 595 nm had different performances with various concentration ranges of GO (Figure 4c and Figure 4d). In Figure 4c, the change of phosphorescence intensity linearly increased with GO concentration from 0 to10.0 mg·L^{-1} with a correlation coefficient of 0.9987 with a calibration function of P-P_0 = 10.87 C+ 1.097 (C in mg·L^{-1}). In Figure 4d, the change of phosphorescence intensity linearly increased with GO concentration from 10.0 to 25.0 mg·L^{-1} with a correlation coefficient of 0.9979 with a calibration function of P-P_0= 60.32 C + 4.919 (C in mg·L^{-1}). Herein, P and P_0 was the phosphorescence intensity of the sensor in the absence and presence of GO, respectively.

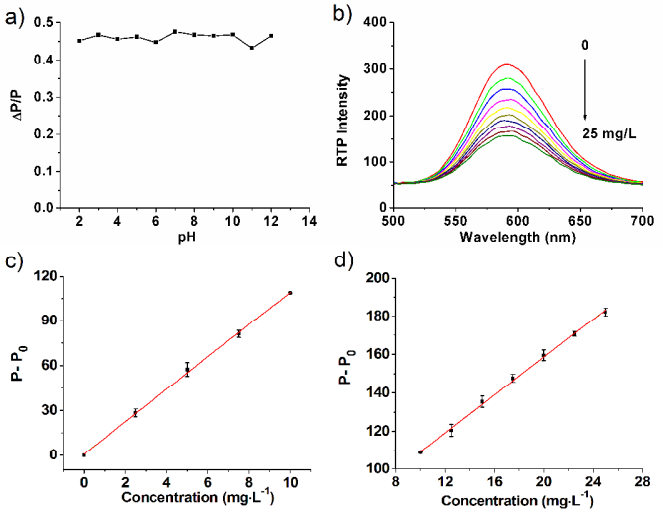

Figure 4. a) Influence of the solution pH of Mn/ZnS@SiO_2-NH_2 on the quenching response of the sensor. b) Phosphorescence spectra of the synthesized Mn/ZnS@SiO_2-NH_2 in the presence of various concentrations of GO. RTP signals of the Mn/ZnS@SiO_2-NH_2 at 595 nm against the concentration of GO from c) 0 to 10.0 mg·L^{-1}, d) 10.0 to 25.0 mg·L^{-1}.

Possible mechanism of the Mn/ZnS@SiO_2-NH_2 for the RTP detection of GO.

The phosphorescence quenching is usually divided into static quenching and dynamic quenching. The dynamic quenching can be described by Stern-Volmer's equation (eq 1) while the static quenching can be described by the Lineweaver-Burk equation (eq 2) [37-38]

$$P_0/P = 1 + K_{SV}C_q \quad (1)$$

$$1/(P_0-P) = 1/P_0 + K_{LB}/(P_0C_q) \quad (2)$$

Where P_0 and P is the phosphorescence intensities of the Mn/ZnS@SiO_2-NH_2 in the absence and in the presence of a quencher, respectively. C_q is the concentration of the quencher, GO. K_{SV} is the dynamic quenching constant, and K_{LB} is the static quenching constant. [39-42] The relationship between (P_0-P) and the concentration of GO shows that the RTP quenching does not follow the Lineweaver-Burk Equation (Figure 5a). However, the linear relationship between ((P_0-P)/P) and the concentration of GO shows that the RPT quenching follows the Stern-Volmer's equation; i.e., dynamic quenching occurs (Figure 5b). These results may imply the formation of non-phosphorescence groundstate complex between the surface of Mn/ZnS@SiO_2-NH_2 nanoparticles and GO.

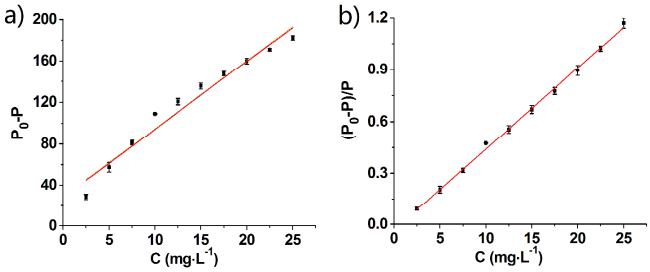

Figure 5. a) Lineweaver–Burk plot and b) Stern-Volmer's plot of RTP quenching of Mn/ZnS@SiO_2-NH_2 by GO.

Application of the Mn/ZnS@SiO_2-NH_2 for RPT detection of GO in environmental water samples.

To validate the practicability of the proposed method, a recovery test of the analysis of spiked water samples from Shahu Lake, East Lake and Changjiang River was carried out. The analytical results were shown in Table 1. The recovery of spiked GO ranged from 98.5% to 107.4%. Thus, our method satisfied the requirements for the detection of GO.

Table 1. Recovery study of spiked water samples

Spiked concentration of GO (mg·L^{-1})	Samples	Found concentration of GO (mg·L^{-1})	Recovery (%)
5.0	Shahu Lake	5.07±0.17	101.3±3.4
5.0	East Lake	4.97±0.04	99.3±0.8
5.0	Changjiang River	5.12±0.25	102.4±5

Conclusions

In summary, we synthesized non-toxic and stable Mn/ZnS@SiO_2-NH_2 nanoparticles and use it as a phosphorescence probe for the detection of GO. Furthermore, the Mn/ZnS@SiO_2-NH_2 RTP-based method was applied to the detection of GO in environmental water samples. This developed Mn/ZnS@SiO_2-NH_2 RTP-based method was non-toxic, cost-effective, label-free, selective and sensitive, which presages more opportunities for application in environmental systems.

Acknowledgement

This work was financially supported by Research Fund for the Doctoral Program of Higher Education of China (20114208120006).

Notes and references

[a]Hubei Collaborative Innovation Center for Advanced Organic Chemical Materials, Wuhan 430062, China
[b]Ministry-of-Education Key Laboratory for the Synthesis and Application of Organic Functional Molecules, College of Chemistry and Chemical Engineering, Hubei University, Wuhan 430062, China

1 K. P. Loh, Q. Bao, G. Eda, M. Chhowalla, *Nat. Chem.,* 2010, **2**, 1015-1024.
2 C. Chung, Y. K. Kim, D. Shin, S. R. Ryoo, B. H. Hong, D. H. Min, *Acc. Chem. Res.*, 2013, **46**, 2211-2224.
3 J. Li, Y. Huang, D. Wang, B. Song, Z. Li, S. Song, L. Wang, L. Jiang, B. Jiang, X. Zhao, J. Yang, R. Liu, D. He, C. Fan, *Chem Commun.*, 2013, **49**, 3125-3127.
4 D. M. Zhou, Q. Xi, M. F. Liang, C. H. Chen, L. J. Tang, J. H. Jiang, *Biosens. Bioelectron.*, 2013, **41**, 359-365.
5 M. Li, W. D. Ding, S. W. Guo, N. Q.Wu, *Biosens. Bioelectron*., 2013, **41**, 889-893.
6 Y. Chang, S. T. Yang, J. H. Liu, E. Dong, Y. Wang, A. Cao, Y. Liu, H. Wang, *Toxicol.Lett.*, 2011, **200**, 201-210.
7 T. Lammel, P. Boisseaux, M. L. Fernandez-Cruz, J. M. Navas, *Part. Fibre Toxicol.*, 2013, **10**, 27.
8 A. Wang, K. Pu, B. Dong, Y. Liu, L. Zhang, Z. Zhang, W. Duan, Y. Zhu, *J. Appl. Toxicol.*, 2013, **33**, 1156-1164.
9 G. Qu, S. Liu, S. Zhang, L. Wang, X. Wang, B. Sun, N. Yin, X. Gao, T. Xia, J. J. Chen, G.B. Jiang, *ACS Nano*, 2013, **7**, 5732-5745.
10 K. H. Liao, Y. S. Lin, C. W. Macosko, C. L. Haynes, *ACS Appl. Mater. Interfaces*, 2011, **3**, 2607-2615.
11 K. Wang, J. Ruan, H. Song, J. Zhang, Y. Wo, S. Guo, D. Cui, *Nanoscale Res. Lett.*,2011, **6**, 8-15.
12 A. I. López-Lorente, B. M. Simonet, M. Valcárcel, *Talanta*, 2013, **105**, 75-79.
13 A. I. López-Lorente, B. M. Simonet, M. Valcárcel, B. Mizaikoff, *Anal. Chim. Acta*, 2013, **788**, 122-128.
14 A. I. López-Lorente, M. L. Polo-Luque, M. Valcárcel, *Anal. Chem.*, 2013, **85**, 10338-10343.
15 L. Li, K. Leopold, *Anal. Chem.*, 2012, **84**, 4340-4349.
16 A. I. López-Lorente, B. M. Simonet, M. Valcárcel, *Analyst*, 2012, **137**, 3528-3534.
17 T. Cheng, D. M. Li, J. Li, B. Ren, G. Wang, J.W. Cheng, *J. Mater. Sci.-Mater El.*, 2015, **26**, 4062-4068.
18 C. Aaron R., M. Igor L., M. J. Matthew, F. Brent R., B. Moungi G., M. Hedi *J. Am. Chem. Soc.*, 2004, **126**, 301-310.
19 Y. He, H. F. Wang, X. P. Yan, *Anal. Chem.* 2008, **80**, 3832-3837.
20 J. M. Traviesa-Alvarez, I. Sa´nchez-Barraga´n, J. M. Costa-Ferna´ndez, R. Pereiro, A. Sanz-Medel, *Analyst*, 2007, **132**, 218-223.
21 C. de Mello Donega´, A. A. Bol, A. Meijerink, *J. Lumin.* 2002, **96**, 87-93.
22 J. H. Chung, J. H. Ah, D. J. Jang, *J. Phys. Chem. B*, 2001, **105**, 4128-4132.
23 B. C. Cheng, Z. G. Wang, *Adv. Funct. Mater.* 2005, **15**, 1883-1890.
24 L. Ozawa, M. Makimura, M. Itoh, *Mater. Chem. Phys.* 2005, **93**, 481-486.
25 S. S. Manoharan, S. Goyal, M. L. Rao, M. S. Nair, A. Pradhan, *Mater.Res. Bull.* 2001, **36**, 1039-1047.
26 S. H. Chen, A. P. Greeff, H. C. Swart, *J. Lumin.* 2005, **113**, 191-198.
27 R. Thakar, Y. C. Chen, P. T. Snee, *Nano Lett.* 2007, **7**, 3429–3432.
28 M. Koneswaran, R. Narayanaswamy, *Sensor Actuat. B-Chem.*, 2009, **139**, 104-109.
29 Y. Q. Wang, T. Zhao, X. W. He, W. Y. Li, Y. K. Zhang, *Biosens. Bioelectron.* 2014, **51**, 40-46.
30 W. S. Hummers, R. E. Offeman, *J. Am. Chem. Soc.* 1958, **80**, 1339-1339.
31 S. Gilje, S. Han, M. S. Wang, K. L. Wang, R. B. Kaner, *Nano Lett.* 2007, **7**, 3394-3398.
32 Y. M. Yang, J. Aw, K. Chen, F. Liu, P. Padmanabhan, Y.L. Hou, Z.Cheng, B.G. Xing, *Chem. Asian J.* 2007, **6**, 1381-1389.
33 R. Kho, C.L. Torres-Marteiz, R.K. Mehra, *J. Colloids Interface Sci.* 2000, **227**, 561-566.
34 T. Somanathan, K. Prasad, K. Ostrikov, A. Saravanan, V. M. Krishna, *Nanomaterials*, 2015, 5, 826-834.
35 A. Esmaeili, M.H. Entezari, *J. Colloid Interf. Sci.*, 2014,432, 19-25.
36 Y. X. Xu, H. Bai, G. W. Lu, C. Li, G. Q. Shi, *J. Am. Chem. Soc.*, 2008, **130**, 5856-5857.
37 K. Sauer, H. Scheer and P. Sauer, *Photochem. Photobiol.* 1987, **46**, 427-440.
38 J. R. Lakowicz and G. Weber, *Biochemistry*, 1973, **12**, 4171-4179.
39 R. M. Jones, T. S. Bergstedt, D. W. McBranch and D. G. Whitten, *J. Am. Chem. Soc.*, 2001, **123**, 6726-6727.
40 C. B. Murphy, Y. Zhang, T. Troxler, V. Ferry, J. J. Martin and W. E. Jones, *Jr, J. Phys. Chem. B*, 2004, **108**, 1537-1543.
41 M. S. Baptista and G. L. Indig, *J. Phys. Chem. B.*, 1998, **102**, 4678-4688.
42 J. R. Lakowicz, Principle of Fluorescence Spectroscopy; 2nd ed.; Plenum Press: New York, 1999.

Figure 1. TEM images of the a) Mn/ZnS QDs, b) Mn/ZnS@SiO_2, c) Mn/ZnS@SiO_2 and d) Mn/ZnS@SiO_2-NH_2.

Figure 2. a) FTIR spectra of the (I) Mn/ZnS QDs, (II) Mn/ZnS@SiO_2 and (III) Mn/ZnS@SiO_2-NH_2. b) Phosphorescence spectrum of the Mn/ZnS@SiO_2-NH_2.

Figure 3. a) XRD pattern and b) FTIR spectrum of GO.

Figure 4. a) Influence of the solution pH of Mn/ZnS@SiO_2-NH_2 on the quenching response of the sensor. b) Phosphorescence spectra of the synthesized Mn/ZnS@SiO_2-NH_2 in the presence of various concentrations of GO. RTP signals of the Mn/ZnS@SiO_2-NH_2 at 595 nm against the concentration of GO from c) 0 to 10.0 $mg \cdot L^{-1}$, d) 10.0 to 25.0 $mg \cdot L^{-1}$.

Figure 5. a) Lineweaver–Burk plot and b) Stern-Volmer's plot of RTP quenching of Mn/ZnS@SiO_2-NH_2 by GO.

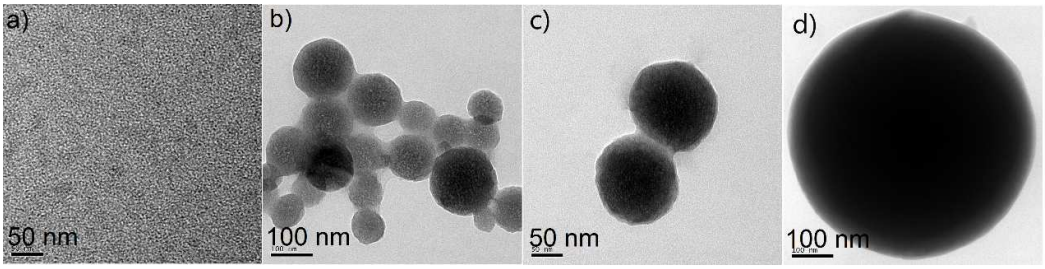

Figure 1. TEM images of the a) Mn/ZnS QDs, b) Mn/ZnS@SiO_2, c) Mn/ZnS@SiO_2 and d) Mn/ZnS@SiO_2-NH_2.

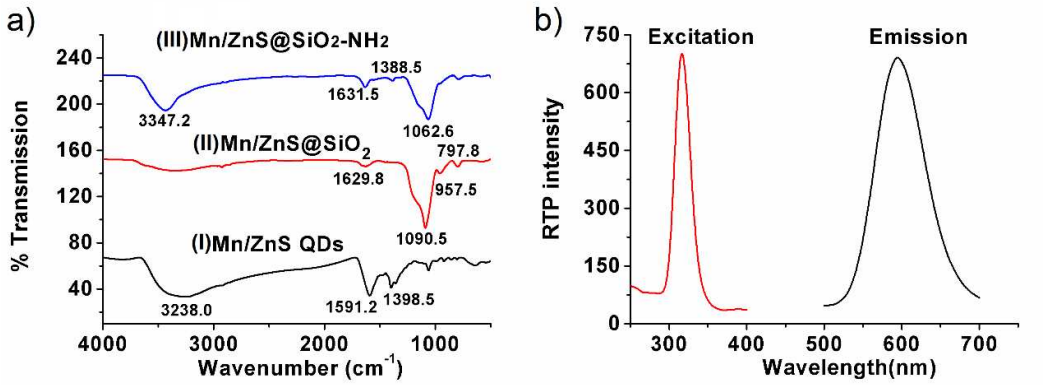

Figure 2. a) FTIR spectra of the (I) Mn/ZnS QDs, (II) Mn/ZnS@SiO_2 and (III) Mn/ZnS@SiO_2-NH_2. b) Phosphorescence spectrum of the Mn/ZnS@SiO_2-NH_2.

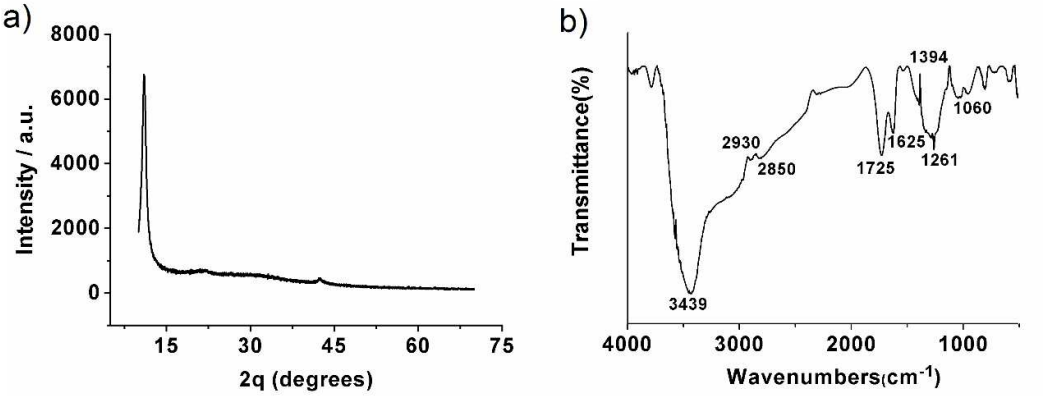

Figure 3. a) XRD pattern and b) FTIR spectrum of GO.

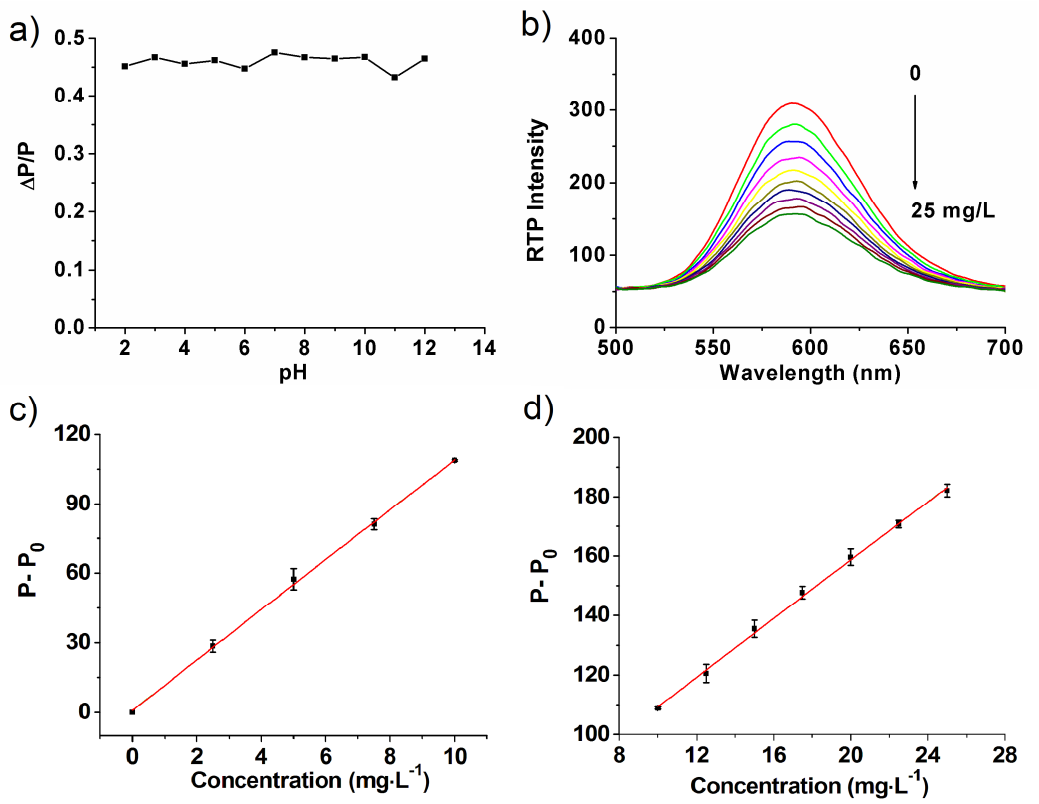

Figure 4. a) Influence of the solution pH of Mn/ZnS@SiO_2-NH_2 on the quenching response of the sensor. b) Phosphorescence spectra of the synthesized Mn/ZnS@SiO_2-NH_2 in the presence of various concentrations of GO. RTP signals of the Mn/ZnS@SiO_2-NH_2 at 595 nm against the concentration of GO from c) 0 to 10.0 mg·L^{-1}, d) 10.0 to 25.0 mg·L^{-1}.

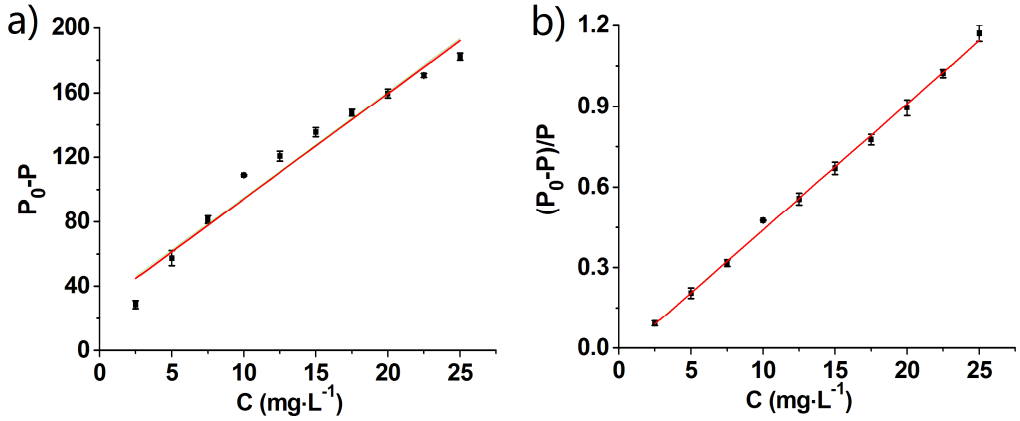

Figure 5. a) Lineweaver–Burk plot and b) Stern-Volmer's plot of RTP quenching of Mn/ZnS@SiO_2-NH_2 by GO.